

FINAL PROJECT REPORT

Project Title:

**Control of Coal Combustion SO₂ and NO_x
Emissions by In-Boiler Injection of CMA.**

DOE Grant #: DE-FG22-92PC92535

Principal Investigator: Yiannis A. Levendis

Graduate Students: Judi Steciak and Ajay Atal

Department of Mechanical Engineering, 334 Snell
Northeastern University, Boston, MA 02115

Consultant: Girard Simons.

Project Performance Period: 1 July 1992 - 31 December 1994

DISCLAIMER

This report was prepared as an account of work sponsored by an agency of the United States Government. Neither the United States Government nor any agency thereof, nor any of their employees, makes any warranty, express or implied, or assumes any legal liability or responsibility for the accuracy, completeness, or usefulness of any information, apparatus, product, or process disclosed, or represents that its use would not infringe privately owned rights. Reference herein to any specific commercial product, process, or service by trade name, trademark, manufacturer, or otherwise does not necessarily constitute or imply its endorsement, recommendation, or favoring by the United States Government or any agency thereof. The views and opinions of authors expressed herein do not necessarily state or reflect those of the United States Government or any agency thereof.

MASTER

DISCLAIMER

**Portions of this document may be illegible
in electronic image products. Images are
produced from the best available original
document.**

Project Objectives:

The principal objectives of this research were two-fold: (A) To understand the mechanism and assess the effectiveness of sulfur capture by the chemical calcium magnesium acetate (CMA); and (B) To evaluate the NO_x reduction capabilities of CMA by pyrolyzing its organic constituent (the acetate) and, thereby, reducing NO to stable N_2 . The optimum conditions and the location of CMA introduction in the furnace were to be identified.

To achieve these goals water solutions of CMA or dry powders of CMA were injected into hot air or gases simulating the furnace exhaust (containing SO_x , NO_x , CO_2 , H_2O , O_2 etc.) and the composition of gaseous and solid products of the reaction was monitored. The processes of burning the organic acetate as well as the calcination, sintering and sulfation of the remaining solids were studied.

The effectiveness of samples of "homemade" CMA, containing various amounts of calcium and magnesium, was investigated to explore the role of these two chemicals in the NO_x and, mainly, in the SO_2 capture processes.

Finally, CMA was introduced in the matrix of coal particles by an ion exchange technique. Upon subsequent combustion, the SO_2 - NO_x emissions were monitored and compared to those from burning untreated coal. The composition and physical structure of the ash residues was examined. Both techniques (CMA pretreatment and CMA injection) may commercially be implemented, either separate or simultaneously. Finally, apart of CMA, the effectiveness of other carboxylic salts of calcium: calcium formate (CF), calcium acetate (CA), calcium propanate (CP) and calcium benzoate (CB) to capture SO_2 and NO_x emissions, in the post-flame region of the furnace, was assessed.

Executive Summary of Contents.

A brief summary of the contents of each chapter in this report is given on page 10, in the section *Outline of the Present Work*.

Overall Abstract

A study was conducted to determine the efficacy of carboxylic calcium and magnesium salts (e.g., calcium magnesium acetate or CMA, $\text{Ca Mg}_2(\text{CH}_2\text{COOH})_6$) for the simultaneous removal of SO_2 and NO_x in oxygen-lean atmospheres. Experiments were performed in a high-temperature furnace that simulated the post-flame environment of a coal-fired boiler by providing similar temperatures and partial pressures of SO_2 , NO_x , CO_2 and O_2 .

When injected into a hot environment, the salts calcined and formed highly porous “popcorn”-like cenospheres. Residual MgO and/or CaCO_3 and CaO reacted heterogeneously with SO_2 to form MgSO_4 and/or CaCO_4 . The organic components – which can be manufactured from wastes such as sewage sludge – gasified and reduced NO_x to N_2 efficiently if the atmosphere was moderately fuel-rich.

Dry-injected CMA particles at a Ca/S ratio of 2, residence time of 1 second and bulk equivalence ratio of 1.3 removed over 90% of SO_2 and NO_x at gas temperatures $\geq 950^\circ\text{C}$. When the furnace isothermal zone was $\leq 950^\circ\text{C}$, Ca was essentially inert in the furnace quenching zone, while Mg continued to sorb SO_2 as the gas temperature cooled at a rate of -130°C/sec . Hence, the removal of SO_2 by CMA could continue for nearly the entire residence time of emissions in the exhaust stream of a power plant.

The composition of the calcined salts was used to interpret the results of a cenosphere sulfation model. The sulfation kinetics of Ca-containing calcined residues were found to be bounded by those of pure CaO and pure CaCO_3 .

The high solubility of the salts makes them excellent candidates for wet injection. Fine mists of CMA sprayed in the furnace at temperatures between 850 and 1050°C , removed 90% of SO_2 at a Ca/S molar ratio of 1, about half of the amount used in the dry injection experiments to achieve a similar SO_2 reduction. The NO_x reduction chemistry was not affected by water when CMA was sprayed at a Ca/S ratio of 1, i.e., the same reduction efficiency was achieved as with dry injection (25 - 30%).

Additional research is needed to improve the efficiency and reduce the cost of the relatively expensive carboxylic acid salts as dual SO_2 - NO_x reduction agents. For example, wet injection of the salts could be combined with less expensive hydrocarbons such as lignite or even polymers such as poly(ethylene) that could be extracted from the municipal waste stream.

List of Publications

1. "The Effectiveness of Calcium Magnesium Acetate (CMA) as an SO_x Sorbent in Coal Combustion" Yiannis A. Levendis, Wenqi Zhu, Donald L. Wise and Girard A. Simons. *AICHE Journal*, **63** (7), 3608, 1993.
2. "Removal of SO_2 by Reaction with Calcium Magnesium Acetate: Comparison of Sulfation Model and Experiment" Judith Steciak, Yiannis A. Levendis and Girard Simons. Presented at the Tenth Annual International Pittsburgh Coal Conference, Pittsburgh, PA, September 20-24, 1993.
3. "The Removal of SO_2 by Calcium Magnesium Acetate of Different Ca to Mg Ratios" Judith Steciak and Yiannis A. Levendis. Presented at the Technical Meeting of the Eastern Sections of the Combustion Institute, Princeton University, Princeton, NJ, October 25-27, 1993.
4. "Calcium Magnesium Acetate (CMA) as an NO_x Reduction Agent in Coal Combustion." J. Steciak, W. Zhu, Y.A. Levendis and D.L. Wise, Presented at the Joint Technical Meeting of the Central and Eastern Sections of the Combustion Institute, New Orleans, LA, March 15-17, 1993.
5. "Combustion and $\text{SO}_2\text{-NO}_x$ Emissions of Bituminous Coal Particles Treated with CMA" Ajay Atal, Judi Steciak and Yiannis A. Levendis. *Fuel*, accepted for publication. 1994.
6. "The Effectiveness of Calcium (Magnesium) Acetate and Calcium Benzoate as NO_x Reduction Agents in Coal Combustion." Judith Steciak, Yiannis A. Levendis and Donald L. Wise. *Combustion Science and Technology*, in the press, 1994.
7. "The Effectiveness of Calcium Magnesium Acetate as a Dual $\text{SO}_2\text{-NO}_x$ Emission Control Agent" Judith Steciak, Yiannis A. Levendis and Donald L. Wise, *AICHE Journal* accepted for publication, 1994.

8. "Dual SO₂-NO_x Concentration Reduction by Calcium Salts of Carboxylic Acids" Judith Steciak, Yiannis A. Levendis, Donald L. Wise and Gerard. *Journal of Environmental Engineering*, accepted for publication, 1994.
9. Wise, D.L., Levendis, Y.A. and Metghalchi, M., co-editors, CMA: An Emerging Bulk Chemical for Multipurpose Environmental Applications, Elsevier Scientific Publishers, the Netherlands, 1991.

Drs. Wise and Levendis have also organized an "International Symposium on Uses of CMA", held at Northeastern University, on 16-19 May, 1991.

Two US Patents have also been issued:

1. "Method of Simultaneously Removing SO₂ and NO_x Pollutants from Exhaust of a Combustion System." U.S. Patent No. 5,312,605, 1994.
2. "Use of Aromatic Salts for Simultaneously Removing SO₂ and NO_x Pollutants from Exhaust of a Combustion System." U.S. Patent No. 5,352,423, 1994.

Table of Contents

	page
Title, Project Objectives	i
Executive Summary	ii
Overall Abstract	iii
List of Publications	iv
Table of Contents	vi
List of Tables	x
List of Figures	xii
Chapter 1. Overall Introduction	1
References	12
Chapter 2. The Effectiveness of Calcium (Magnesium) Acetate and Calcium Benzoate as NO_x Reduction Agents in Coal Combustion	15
References	47
Chapter 3. The Effectiveness of Calcium Magnesium Acetate as a Dual SO₂-NO_x Emission Control Agent	53
References	88
Chapter 4. Dual SO₂-NO_x Reduction by Fine Mists of CMA	94
References	120
Chapter 5. Dual SO₂-NO_x Reduction by Calcium Salts of Carboxylic Acids	122
References	178

Chapter 6. Custom-Blended Secondary Fuel and Sorbent Injection for Dual SO₂-NO_x Emission Control	183
References	201
Chapter 8. Overall Summary	203
Appendix I. Combustion and SO₂-NO_x Emissions of Bituminous Coal Particles Treated with CMA	207
References	243
Appendix II. Determination of the Bulk Equivalence Ratio, ϕ	246
Appendix III. Chemical Thermodynamics and Chemical Kinetics Calculations	251

List of Tables

Table 2.I Bulk Equivalence Ratio, ϕ	30
Table 2.II Residue Colors	33
Table 2.III Possible NO Reduction Reactions, Equilibrium Constants and Reaction Rate Constants at 1130°C	40
Table 2.IV Possible Reactions Involving the Phenyl Radical Equilibrium Constants and Reaction Rate Constants at 1130°C	41
Table 3.I Nominal vs. Actual Mole Percentage of Ca	74
Table 3.II SO ₂ Reduction in the Isothermal Zone and in the Post-Furnace Zone	77
Table 3.III Relative Contribution of Ca and Mg in CMA to SO ₂ Reduction in the Isothermal Zone	77
Table 3.IV Ca and Mg Utilization in the Isothermal Zone	78
Table 3.V XRD Analysis of Sulfated CMA Residues	80
Table 4.I Dual SO ₂ -NO _x Reduction at Gas Temperatures near 1050°C	115
Table 5.I Physical Characteristics of Sorbents after Calcination at 950°C	144
Table 5.II Effect of Afterfire Air on SO ₂ /NO _x Reduction	152
Table 5.III Mass Percentages of CaCO ₃ and CaO in Calcined CP	171
Table 5.IV Kinetic Data for Sulfation Reactions	172
Table 5.V Calculated Apparent Shell Density and Porosity	178

Table 6.I SO ₂ -NO _x Reduction by CP and Lignite at 1050°C	192
Table 6.II SO ₂ -NO _x Reduction by CF and Sucrose at 1000°C	195
Table 6.III SO ₂ -NO _x Reduction by CF and Poly(ethylene)	198
Table I.I Properties of the Coals Used	218
Table I.II Physical Properties of the PSOC-1451 Coal and Char	220
Table I.III Emissions of SO ₂ and NO _x from Pulverized Coal	235

List of Figures

Figure 1.1 A schematic of staged combustion for NO_x control in a pulverized coal boiler. Courtesy of Mitsubishi Heavy Industries, LTD. 7

Figure 1.2 A Schematic of post-combustion injection of secondary fuel in a coal-fired boiler. Courtesy of Mitsubishi Heavy Industries, LTD. 8

Figure 2.1 High Temperature Furnace, Particle Fluidizer, Pyrometer and Gas Monitoring System 2

Figure 2.2 Residues from NO Reduction Experiments With Calcium Magnesium Acetate and 500 ppm NO

- a. Unreacted, 53-63 μm
- b. 750 $^{\circ}\text{C}$, 0% O_2
- c. 950 $^{\circ}\text{C}$, 0% O_2
- d. 1150 $^{\circ}\text{C}$, 0% O_2
- e. 750 $^{\circ}\text{C}$, 2% O_2
- f. 1150 $^{\circ}\text{C}$, 2% O_2
- g. 750 $^{\circ}\text{C}$, 5% O_2
- h. 1150 $^{\circ}\text{C}$, 5% O_2

25

Figure 2.3 NO Reduction by CMA at various gas temperatures, o— -- o 0% O_2 ; x—x 2% O_2 ; *— ·—* 5% O_2 27

Figure 2.4 NO Reduction by CA at various gas temperatures, o— -- o 0% O_2 ; x—x 2% O_2 ; *— ·—* 5% O_2 28

Figure 2.5 NO Reduction by CB at various gas temperatures, o— -- o 0% O_2 ; x—x 2% O_2 ; *— ·—* 5% O_2 29

Figure 2.6 Calcium Benzoate Combustion in Reduced Oxygen. a) Combustion Intensity in 5% O_2 . b) Combustion Temperature in 5% O_2 . c)

Combustion Intensity in 2% O₂. d) Combustion Temperature
in 2% O₂. 38

Figure 2.7 NO_x reduction (%) or NH₃ concentration (ppm) as a function of
gas temperature. Data from both the isothermal and afterfire
air zones. 43

Figure 2.8 Threshold of NH₃ formation in isothermal and afterfire air zones.
Bulk ϕ of isothermal zone at which 5 ppm NH₃ was detected vs. gas
temperature. 45

Figure 3.1 SEM of calcined CMA. Porosity = 0.70, BET=25-30 m²/g when
calcined at 950°C. 59

Figure 3.2 SEM of calcined CMA particle cracked open to reveal interior
voids and pore structure. 60

Figure 3.3 Schematic of the high temperature furnace, particle fluidizer, and
gas monitoring system. 62

Figure 3.4 Typical temperature-time histories of sorbents from entry into
the isothermal zone (time 0), to exit from the isothermal zone and entry
into the post-furnace -130°C/sec. quenching zone (at about 4.5 sec; this
was also the point where the nitrogen-quenched water-cooled quenching
probe was inserted). 64

Figure 3.5 TGA profiles for CMA, CA and MA. Heating rate was 20°C/min.
Rate of mass loss in mg/s. 66

Figure 3.6 SO₂ and NO_x reduction by CMA as a function of temperature at
Ca/S=2 ((Ca+Mg)/S=6) in atmospheres containing 12% CO₂, 3% O₂,
2000 ppm SO₂ and 1000 ppm NO. 1 s residence time. o - SO₂ reduction;
x - NO_x reduction. a) Without after-fire air; b) With after-fire air. 67

Figure 3.7 SO_2 and NO_x reduction by CMA as a function of temperature at $\text{Ca}/\text{S}=2$ ($(\text{Ca}+\text{Mg})/\text{S}=6$) in atmospheres containing 3% O_2 , 2000 ppm SO_2 and 1000 ppm NO. o - SO_2 reduction at 4 to 5 sec. residence time; * - SO_2 reduction at 2 to 3 sec. residence time; x - NO_x reduction at 2 to 3 sec. residence time. 68

Figure 3.8 SO_2 and NO_x reduction by CA as a function of temperature at $\text{Ca}/\text{S}=2$ in atmospheres containing 3% O_2 , 2000 ppm SO_2 and 1000 ppm NO. o - SO_2 reduction; x - NO_x reduction. Nominal furnace residence time varied between 4 to 5 sec. 70

Figure 3.9 SO_2 and NO_x reduction by MA as a function of temperature at $\text{Mg}/\text{S}=4$ in atmospheres containing 3% O_2 , 2000 ppm SO_2 and 1000 ppm NO. o - SO_2 reduction; x - NO_x reduction. Nominal furnace residence time varied between 4 to 5 sec. 72

Figure 3.10 SO_2 and NO_x reduction by CMA with different Ca-to-Mg molar ratios at a temperature of 950°C in atmospheres containing 3% O_2 , 2000 ppm SO_2 and 1000 ppm NO. 100% Ca corresponds to calcium acetate, 0% Ca is 100% Mg or magnesium acetate, and commercial CMA is about 30% Ca. o - SO_2 reduction; x - NO_x reduction. 73

Figure 3.11 SO_2 reduction by rapidly quenched reactions as a function of temperature with $\text{Ca}/\text{S}=2$ or $\text{Mg}/\text{S}=4$ in atmospheres containing 3% O_2 , 2000 ppm SO_2 and 1000 ppm NO. o - CMA; * - CA; • - MA. Nominal furnace residence time varied between 4 to 5 sec. NO_x reduction was not affected by quenching. 76

Figure 4.1 Experimental apparatus. 99

Figure 4.2 SEM photograph of sprayed CMA sulfated at 750°C. Low magnification 102

Figure 4.3 SEM photograph of sprayed CMA sulfated at 750°C. High magnification. Note cenospheres with extremely thin, porous walls.	103
Figure 4.4 SEM photograph of sprayed CF sulfated at 1050 °C. Low magnification.	104
Figure 4.5 SEM photograph of sprayed CF sulfated at 1050 °C. High magnification.	105
Figure 4.6 SEM photograph of sprayed CA sulfated at 1050 °C. Low magnification.	106
Figure 4.7 SEM photograph of sprayed CA sulfated at 1050 °C. High magnification.	107
Figure 4.8 SEM photograph of sprayed CP sulfated at 1050 °C. Low magnification.	108
Figure 4.9 SEM photograph of sprayed CP sulfated at 1050 °C. High magnification.	109
Figure 4.10 Dual SO ₂ -NO _x reduction by CMA as a function of temperature in atmospheres containing 3% O ₂ , 2000 ppm SO ₂ , and 1000 ppm NO in N ₂ . SO ₂ reduction by wet and dry injection at Ca/S=1.	111
Figure 4.11 Dual SO ₂ -NO _x reduction by CMA. NO _x reduction by wet and dry injection at Ca/S=1.	112
Figure 4.12 Dual SO ₂ -NO _x reduction by CMA. SO ₂ reduction by wet and dry injection at Ca/S=2.	113
Figure 4.13 Dual SO ₂ -NO _x reduction by CMA. NO _x reduction by wet and dry injection at Ca/S=2.	114
Figure 5.1 SEM of unreacted calcium formate	126

Figure 5.2 SEM of calcined CF sulfated at 1225 K. Note formation of cylindrical protrusions.	127
Figure 5.3 SEM of calcined CF, cracked open to reveal interior voids and grainy shell structure.	128
Figure 5.4 SEM of unreacted calcium acetate. Note the brittle, elongated crystals of about $10\mu\text{m}$ in length and a few μm in width.	129
Figure 5.5 SEM of calcined CA sulfated at 1175 K. The unreacted crystals have coalesced into spheres.	130
Figure 5.6 SEM of calcined CA, cracked open to reveal interior void and thin porous shell.	131
Figure 5.7 SEM of unreacted calcium propionate.	132
Figure 5.8 SEM of calcined CP sulfated at 1025 K.	133
Figure 5.9 SEM of calcined CA, cracked open to reveal interior voids and grainy shell structure.	134
Figure 5.10 SEM of glassy cenosphere, cracked open to reveal thin, comparatively non-porous thin shell.	135
Figure 5.11 SEM of unreacted calcium benzoate. Note brittle, elongated crystals of $10\mu\text{m}$ in width and $30 - 50\mu\text{m}$ in length.	136
Figure 5.12 SEM of CB after calcination in air at 1275 K. Note large blowholes on surface.	137
Figure 5.13 Calcined CB cracked open to reveal cenospheric structure and shell porosity.	138
Figure 5.14 Experimental apparatus.	140

Figure 5.15 TGA profiles for CF, CA, CP and calcium carbonate. Rate of mass loss is in mg/s. 142

Figure 5.16 TGA profiles for CB. Rate of mass loss is in mg/s. 144

Figure 5.17 Pore volume distribution of sorbents calcined at gas temperatures between 750-950°C in 3% O₂. — CF; - - - CA; - - - CF. 146

Figure 5.18 Pore surface-area distribution of sorbents calcined at gas temperatures between 750-950°C in 3% O₂. — CF; - - - CA; - - - CF. The differently-scaled inset shows the predominance of small pores in CA. 147

Figure 5.19 Removal of SO₂ as a function of temperature in atmospheres containing 2000 ppm SO₂, 1000 ppm NO, 3% O₂ in N₂ with containing 2000 ppm SO₂, 1000 ppm NO, 3% O₂ in N₂ with Ca/S = 3.1. a) SO₂ reduction. o without after-fire air; * with after-fire air; \otimes , o 12% CO₂ added. b) NO_x reduction. x without after-fire air; + with after-fire air; \oplus , \otimes 12% CO₂ added. 149

Figure 5.20 Removal of SO₂ as a function of temperature in atmospheres containing 2000 ppm SO₂, 1000 ppm NO, and 3% O₂ in N₂ with Ca/S molar ratios ranging between 2.4 and 3.1. o CF; x CA; * CP; \oplus CB. 150

Figure 5.21 Reduction of NO_x as a function of temperature in atmospheres containing 2000 ppm SO₂, 1000 ppm NO, and 3% O₂ in N₂ with Ca/S molar ratios ranging between 2.4 and 3.1. o CF; x CA; * CP; \oplus CB. 151

Figure 5.22 SO₂ reduction as a function of bulk ϕ , including changes in SO₂ reduction due to the addition of afterfire air. o CF; x CA; * CP; \oplus CB. — 950°C; - - - 750°C. 154

Figure 5.23 NO_x reduction as a function of bulk ϕ , including changes in NO_x reduction due to the addition of afterfire air. o CF; x CA; * CP; \oplus CB. 156

Figure 5.24 Calcium utilization as a function of temperature in atmospheres containing 2000 ppm SO_2 , 1000 ppm NO, and 3% O_2 in N_2 with Ca/S molar ratios ranging between 2.4 and 3.1. o CF; x CA; * CP; \oplus CB. 158

Figure 5.25 Changes in Ca utilization as a function of temperature due to the addition of afterfire air. o CF; x CA; * CP; \oplus CB. 159

Figure 5.26 Ca utilization as a function of bulk ϕ , including changes in utilization due to the addition of afterfire air. o CF; x CA; * CP; \oplus CB. — 950°C; - - - 750°C. 160

Figure 5.27 The Pore Tree 163

Figure 5.28 Ca utilization vs. temperature, comparison of model calculation and experimental measurements. o data; - - - model using CaCO_3 ; — model using CaO ; - - - model fit to data. 167

Figure 5.29 Percentage of Ca retained as CaCO_3 in calcined sorbents. o CF; x CA; * CP; + pure CaCO_3 (CC). 169

Figure 5.30 Sulfation kinetics of different sorbents. o CF; x CA; * CP; — CaCO_3 ; - - - CaO . Pre-exponential factors and activation energies are listed in Table IV. 173

Figure 6.1 Photograph of the experimental apparatus 190

Figure 6.2 Ca Utilization by CF and sucrose as a function of ϕ at 1000°C 196

Figure 6.3 NO _x Reduction by CF and sucrose as a function of ϕ at 1000°C	197
Figure I.1 SEM micrograph of plain pulverized coal.	216
Figure I.2 SEM micrograph of pulverized coal treated with CMA.	217
Figure I.3 Schematic of the furnace with the axial gas temperature profile and trajectory of burning particles	219
Figure I.4 SEM micrograph of plain pulverized coal after pyrolysis in nitrogen at $T_g = 1450\text{K}$. Low magnification.	223
Figure I.5 SEM micrograph of plain pulverized coal after pyrolysis in nitrogen at $T_g = 1450\text{K}$. High magnification.	224
Figure I.6 SEM micrograph of CMA-treated pulverized coal after pyrolysis in nitrogen at $T_g = 1450\text{K}$. Low magnification.	225
Figure I.7 SEM micrograph of CMA-treated pulverized coal after pyrolysis in nitrogen at $T_g = 1450\text{K}$. High magnification.	226
Figure I.8 Three-color pyrometry intensity signals (top row) and two-color ratio temperature profiles (bottom row) for burning pulverized plain coal particles (75-90 μm) in air at T_g of 1450K. High-speed cinematography frames of some burning pulverized coal particles in air at T_g of 1450K are included.	228
Figure I.9 Three-color pyrometry intensity signals (top row) and two-color ratio temperature profiles (bottom row) for burning aggregates of micronized coal particles in air at T_g of 1450K. Frames from the high-speed cinematography are attached next to the traces	231

Figure I.10 Three-color pyrometry intensity signals (top row) and two-color ratio temperature profiles (bottom row) for burning pulverized CMA-treated coal particles (75-90 μm) in air at T_g of 1450K 232

Figure I.11 Three-color pyrometry intensity signals (top row) and two-color ratio temperature profiles (bottom row) for burning pulverized CA- and MA-treated coal particles (75-90 μm) in air at T_g of 1450K 234

Figure I.12 SO_2 (—) and NO_x (---) emissions from pulverized (PSOC 1451, 75-90 μm) coal with and without sorbent treatment burning at 1450K. (i) plain; treated with (ii) CMA, (iii) CA, (iv) MA. 236

Figure I.13 SO_2 (—) and NO_x (---) emissions from micronized (Otisca, 4 μm) coal with and without sorbent treatment burning at 1450K. (i) plain; treated with CMA burning in (ii) air, (iii) 40% O_2 . 237

Figure I.14 SO_2 (—) and NO_x (---) emissions from pulverized (PSOC 1451, 75-90 μm) coal with and without sorbent treatment burning at 1450K. (i) plain, sample extracted at the end of the isothermal zone; (ii) with CMA, sample extracted at the end of the isothermal zone; (iii) plain, sample extracted at the mid-height of the isothermal zone; (iv) with CMA, sample extracted at the mid-height of the isothermal zone. 239

CHAPTER 1.

Overall Introduction

1 Problem Statement

Emissions of SO_2 and NO_x ($\text{NO} + \text{NO}_2$) from stationary combustion sources contribute to acid rain formation in the atmosphere; NO_x also contributes to the formation of urban smog and to the depletion of stratospheric ozone. Over half of the electricity generated in the USA is produced from the combustion of coals in plants that are major producers of SO_2 and NO_x . Vast reserves of coal are found in the USA and developing nations such as China and, indeed, coal is the most abundant fossil fuel in the world. It is expected that coal will continue to be used for fuel for a substantial length of time and that concerns relative to effective control of SO_2 and NO_x will continue well into the future.

At present, the control of sulfur and nitrogen oxide emissions from coal-fired power plants is achieved with separate processes often in multiple stages.

1.1 Methods of Sulfur Reduction.

Methods of reducing sulfur emissions can be placed in four general categories: 1) fuel substitution; 2) fuel desulfurization; 3) combustion process modification; and 4) desulfurization of combustion products.

1) Fuel Substitution. The sulfur content of different types of coals varies between 0.5 to 4%. Substituting a low-sulfur coal for a high-sulfur coal will reduce sulfur emissions accordingly.

2) Fuel Desulfurization. Coal can be physically cleaned. Efforts to remove ash-forming compounds by physically crushing coal and then separating mineral impurities from the organic coal also remove some of the sulfur. Sulfur bounds organically to the coal substrate and inorganically with iron particles

(pyrite) and it is the pyritic sulfur that is removed. Typically, 40% reduction in sulfur can be achieved by mechanical cleaning (EPA, 1981).

3) Combustion Process Modification. Compounds containing Ca and Mg – most often limestone or dolomite – can be added to coal during combustion to react with fuel sulfur as it is released. For example, limestone can be added to coal burning in a fluidized bed, where the temperature is high enough to calcine the stone (800 – 900°C) and create a more porous solid, but low enough to preclude both the dissociation of the resulting sulfate and/or sintering of the calcined stone. First, limestone calcinates:



SO_2 then reacts heterogeneously with the calcined stone. In an oxygen-rich atmosphere:



In an oxygen-lean atmosphere:



If the temperature is below the decomposition temperature of the carbonate, SO_2 can also react directly with CaCO_3 :



Calcium-based sorbents also have been added to coal by ion-exchange (Freund and Lyon, 1982) and by wetting pulverized and micronized coals with aqueous solutions of calcium magnesium acetate, calcium acetate and magnesium acetate (Atal, et al., 1994; Appendix 1).

4) Desulfurization of Combustion Products. Electric utilities in the USA rely on flue gas desulfurization (FGD) to control SO_2 emissions for their newer facilities. FGD processes are either wet or dry (referring to the state of FGD products removed for disposal or regeneration) and wet systems dominate in the USA (EPA, 1981) and Japan (Ando, 1985) as well as Europe. FGD processes are also either regenerative (sulfur is separated from the spent

sorbent which can then be reused) or throwaway (the sulfur-sorbent product is discarded).

For example, the most widely used flue gas desulfurization strategies involve wet or dry scrubbing with non-regenerated calcium compounds such as slaked lime or limestone slurries. Injection of these sorbents in the high-temperature boiler gases also has received much attention because of the projected low capital investment. As an example of in-boiler sorbent injection, Cole, et al. (1986) reported that hydrated materials (e.g., slaked lime) were more reactive than limestone, and that dolomitic sorbents were more reactive than calcitic sorbents. They attributed the differences in reactivities to the higher surface area of hydrated sorbents compared to carbonic sorbents, and to the higher surface area of dolomitic sorbents compared with calcitic sorbents. For example, a mean surface area of $\approx 50 \text{ m}^2/\text{g}$ was measured for hydrated dolomitic sorbents compared with an average of $\approx 25 \text{ m}^2/\text{g}$ for hydrated calcitic sorbents. This resulted in average Ca utilizations of $\approx 26 \%$ and $\approx 16 \%$, respectively, for hydrated dolomitic and calcitic sorbents exposed to 2000 ppm SO₂ at $\approx 1100^\circ\text{C}$ for 0.5 sec. with a Ca/S molar ratio of 2 (Cole, et al., 1986). The correlation of SO₂ reduction with sorbent surface area was also reported by Greene, et al. (1985) and the high surface area of dolomite was given as a reason for its high sulfur affinity. Evidence of pore structure was also reported to influence sulfation rates, with the plate-like pores of CaO from hydrated sorbents posing less diffusional resistance when compared to the sphere-shaped pores of CaO from calcitic sorbents (Bruce, et al., 1989).

Processes using magnesium are examples of regenerative FGD methods. At temperatures between 40 to 65°C, magnesium hydroxide slurries react with SO₂ to form hydrated magnesium sulfites ($\text{MgSO}_3 \bullet 3\text{H}_2\text{O}$ or $\text{MgSO}_3 \bullet 6\text{H}_2\text{O}$). The sulfites are dried and calcined to recover MgO and SO₂ for production of sulfuric acid or elemental sulfur (EPA, 1981; Flagan and Seinfeld, 1988).

The low-temperature reactions between Mg and S compounds may be an additional reason why utilities report improved SO_2 removal when MgO is added to lime slurries (EPA, 1981).

1.2 Methods of NO_x Reduction.

For utility boilers in the USA, 50% of the NO_x emissions are attributed to coal combustion (EPA, 1983). Current NO_x reduction strategies fall into one of two categories: either 1) suppression of NO_x formation during combustion; or 2) removal of NO_x from the stack. Fuel substitution is not as practical as it is for SO_2 reduction because NO_x can also be generated from atmospheric nitrogen. Moreover, the nitrogen content of coals is fairly consistently ≈ 1.5 wt. %, thus, it is not possible to substitute a low-nitrogen coal.

1) **Suppression of NO_x Formation.** To understand how altering operating conditions of a furnace controls NO_x , it is necessary to understand how NO_x is formed during combustion. In coal combustion, NO emissions dominate NO_x emissions and NO readily oxidizes to NO_2 at ambient conditions outside the stack.

Atmospheric nitrogen can form NO during combustion by two mechanisms: thermal fixation at high temperatures near stoichiometric combustion (“thermal-NO”) (Zeldovich et al., 1947, in Flagan and Seinfeld, 1988; Hanson and Saliman, 1984); and low-temperature, fuel-rich, short residence-time formation (“prompt-NO”) (Fenimore, 1971, in Flagan and Seinfeld, 1988; Bowman, 1975). Organically bound heterocyclic nitrogen compounds in coal also oxidize to NO during combustion (“fuel-NO”) (Sarofim and Flagan, 1976) and create most of the NO_x emissions from coal (Beér, 1988).

Thermal-NO formation is sensitive to temperature and this characteristic is exploited in control strategies. Reducing the temperature to slow the rate of N_2 oxidation can be achieved by low excess air firing, flue gas recirculation,

and staging combustion so that a cooler, slower-burning, fuel-rich flame is followed by overfire air (Figure 1). Since the oxidation of fuel nitrogen is more sensitive to stoichiometry than temperature, staged combustion (a fuel-rich zone is followed by a fuel-lean zone) also controls fuel-NO. Low- NO_x burners reduce the mixing rate between coal and air, providing the time required for N_2 formation. The most popular NO_x control methods for USA coal-fired utility boilers are staged combustion or low- NO_x burners (EPA, 1983).

However, present combustion modifications may be approaching the limit of their NO_x reduction capabilities and these techniques alone are insufficient, at times, to meet the regulations for NO_x emissions from coal-fired boilers. For example, combustion modifications from tangential and wall-fired boilers have resulted in NO_x emissions of 220 – 440 ppm (at 3% oxygen) whereas NO_x emission regulations for coal-fired boilers are between ≈ 100 – 360 ppm at 6% O_2 or 80 to 300 ppm at 3 % O_2 (Bowman, 1992). Hence, to remove a sufficient amount of NO_x , it will be necessary to use some post-combustion treatment.

2) Post-Combustion Removal of NO_x . The major post-combustion NO_x emissions destruction methods are 1) selective non-catalytic reduction (SNCR) and selective catalytic reduction (SCR) wherein nitrogen-containing compounds (e.g., ammonia (Lyon, 1974) and urea (Arand, et al., 1982)) are injected downstream of the boiler; and 2) injection of secondary fuels in a fuel-rich zone downstream of the primary combustion zone (Myerson, 1975; Figure 2).

NO_x reductions of 80 – 90% have been reported for SNCR and SCR at a RN/NO molar ratio of 2. However, N_2O and SO_3 (if SO_2 is present) may be released depending on the type of catalyst used in SCR. NH_3 may be released depending on the amount of ammonia slip in SNCR (Bowman, 1992).

When a secondary fuel such as methane is injected to create a fuel-rich zone, CH_4 radicals react with NO to reduce it to N_2 . The reaction paths include

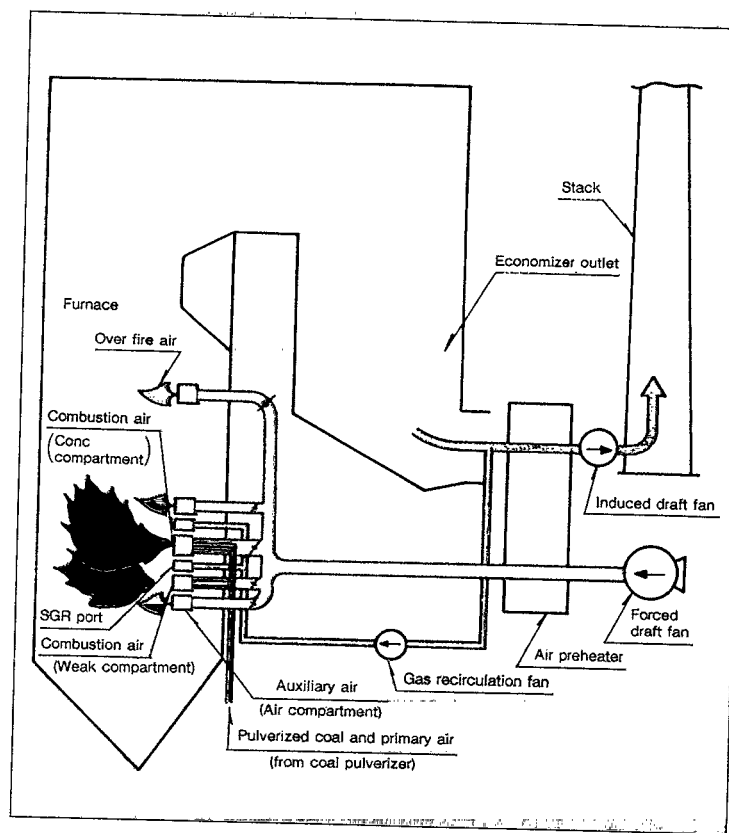


Figure 1: A schematic of staged combustion for NO_x control in a pulverized-coal boiler. Courtesy of Mitsubishi Heavy Industries, LTD.

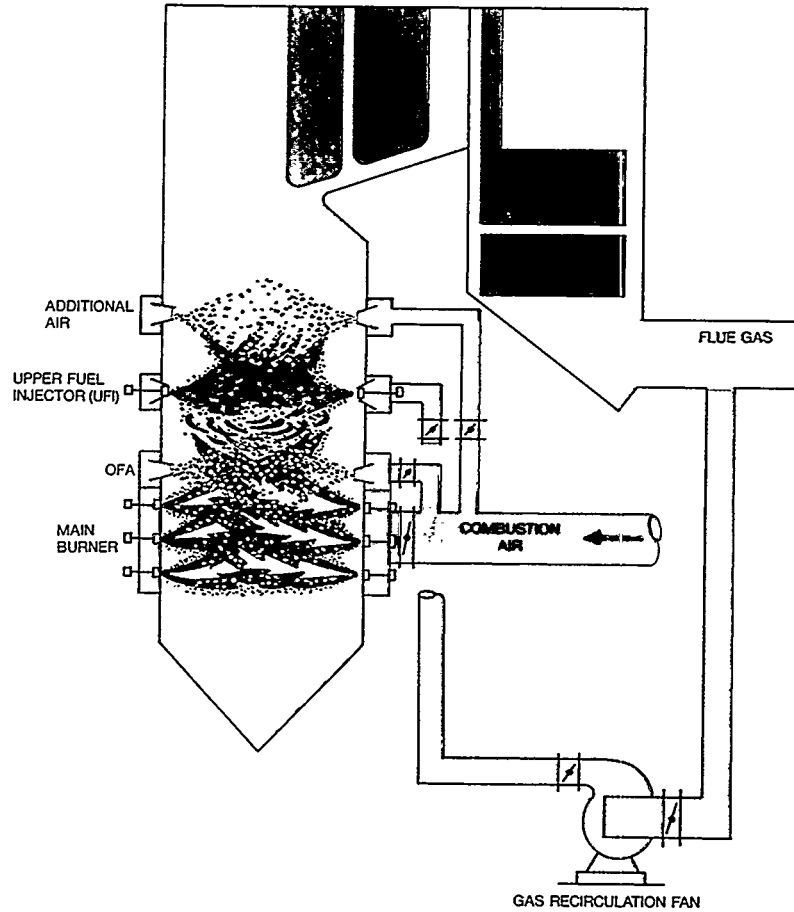


Figure 2: A schematic of post-combustion secondary fuel injection for NO_x control in a coal-fired boiler. Courtesy of Mitsubishi Heavy Industries, LTD.

the formation of CH and NH compounds and are similar to those followed in prompt-NO and fuel-NO (Beér, 1988; Miller and Bowman, 1989). Injection of air after the fuel-rich zone completes the oxidation of CO, unburned hydrocarbons, and any small amount of HCN or NH₃ (Myerson, 1975). In coal-fired furnaces, NO_x reduction efficiencies of 70% for cyclone-fired boilers (Yagiela, et al., 1991) and 40 – 50 % for wall-fired and tangentially-fired boilers (Bowman, 1992) have been reported when natural gas was used as the secondary fuel. NO_x reductions of 60% were reported for a pilot-scale furnace using pulverized coal as the secondary fuel (Bowman, 1992).

1.3 Dual SO₂-NO_x Control.

If control of both pollutants is desired, the current strategy is simply to combine separate SO₂ and NO_x removal processes, e.g., low-NO_x burners are combined with wet or dry desulfurization by using throwaway calcium compounds such as slaked lime or limestone slurries. Few processes exist where one control agent is used for the simultaneous removal of SO₂ and NO_x.

This research is a study of the control of SO₂ and NO_x emissions from coal combustion by post-combustion injection of carboxylic salts. The process could be classified as the injection of a secondary fuel to control NO_x occurring simultaneously with the wet or dry injection of a non-regenerative SO₂ sorbent. The study is based on laboratory-scale experiments in a high temperature furnace. The furnace simulates the post-combustion environment in coal-fired boilers by achieving similar temperatures and concentrations of SO₂, NO, and O₂. While most of the nitrogen oxide emission from coal combustion is in the form of NO, some NO may oxidize to NO₂ in the furnace, hence, the total reduction of both oxides, NO_x, was actually measured in the experiments. The emphasis of this research was on developing an understanding of the mechanisms of SO₂ and NO_x removal, optimizing the temperature and rate of

sorbent injection that achieved the most efficient reduction, and investigating the presence of additional pollutants, such as CO, H₂S, HCN, NH₃ and N₂O, that may be created from reactions between the salts, SO₂ and NO.

Why are carboxylic calcium and magnesium salts candidate agents for the simultaneous removal of the pollutants SO₂ and NO_x from the effluent of coal-fired stationary boilers? The unique chemical structure of the salts – a combination of alkaline earth metals and organic hydrocarbons – is the key to their efficacy as dual SO₂-NO_x reducing agents. When the salts are injected into a hot environment containing SO₂ and NO_x (e.g., in a boiler just downstream of the primary combustion burner), they calcine, releasing hydrocarbon radicals and leaving behind porous cenospheres of CaCO₃, CaO or MgO. The carbonate and oxides react with SO₂ to form CaSO₄ and MgSO₄. In the oxygen-lean atmosphere, the hydrocarbon radicals react with NO to form N₂. In addition, CaO can act as a catalyst during the reduction of NO.

2 Outline of Present Work

The unique capability of CMA and other carboxylic salts to serve as dual SO₂ and NO_x reducing agents has not been explored by other investigators. Previous work in oxidizing atmospheres (Levendis, et al., 1993) identified the encouraging SO₂ sorption characteristics of CMA and CA compared to traditional SO₂ sorbents including calcium hydroxide (slaked lime) and calcium carbonate (limestone). The next step was to determine the efficiency of the carboxylic salts as NO_x reduction agents by injecting them into reducing atmospheres containing NO (Chapter 2).

Chapter 3 presents the results from dry-injection dual SO₂-NO_x reduction experiments – the focus of this research. The contribution of Mg to SO₂

preprints removed
AS

reduction was quantified. Other aspects of the dual SO_2 - NO_x reduction process are addressed in subsequent chapters.

The high solubility of the salts permits their injection as solutions. Fine mists – and subsequently small aerosols of CaO and MgO – are thus obtained and promote more efficient heterogeneous reaction between gaseous SO_2 and the solid oxides (Chapter 4). *conf cycled separately* BS

preprint removed. The importance of the organic hydrocarbons on SO_2 - NO_x reduction was explored in Chapter 5 by simultaneous SO_2 - NO_x reduction experiments using carboxylic calcium salts with different amounts of aliphatic hydrocarbons (formate, acetate and propionate). The importance of organic structure was explored using a calcium salt with an aromatic hydrocarbon (calcium benzoate). Calcium utilizations obtained experimentally were compared to utilizations calculated with a cenospheric sulfation model.

Commercial sources of carboxylic salts are expensive due to the manufacture of the acid (formic, acetic, or propionic) from natural gas. Alternatives to reduce cost include manufacture of the acids from biomass, sewage sludge, or even – in the case of benzoic acid – from coal, and improving the utilization of the alkali earth metals while combining them with other sources of less expensive hydrocarbon fuels, including lignite. Chapter 6 presents some of these carboxylic salt combinations, enhancers and “analogs” that may provide a cost-effective solution to simplify SO_2 and NO_x removal from existing power plants. This chapter also presents calculations to illustrate the economics of different SO_2 - NO_x reduction schemes.

Chapter 7 summarizes the most important findings of this investigation and presents recommendations for future research.

While the main purpose of this work was the study of post-combustion injection of sorbents for removal of SO_2 and NO_x , Appendix 1 describes experiments in conjunction with a separate project that were performed to

assess the efficacy of pre-treating coal with carboxylic acid salts. In these experiments, coal particles of different size and sulfur content were treated with CMA, CA and MA. Treated and untreated particles were burned in air at the temperatures expected in pulverized coal burners. Virtually no SO_2 was detected during the combustion of treated pulverized coal particles.

Appendices 2 and 3 contain example calculations of equivalence ratios, chemical thermodynamics and chemical kinetics.

3 References

- -, "Control Techniques for Sulfur Oxide Emissions from Stationary Sources - Second Edition," EPA-450/3-81-004, U. S. Environmental Protection Agency, Research Triangle Park, NC, April, 1981.
- -, "Control Techniques for Nitrogen Oxides Emissions from Stationary Sources - Revised 2nd Edition," EPA-450/3-83-002, U. S. Environmental Protection Agency, Research Triangle Park, NC, January, 1983.
- Ando, J., "Recent Developments in SO_2 and NO_x Abatement Technology for Stationary Sources in Japan," EPA/600/S7-85/040, U. S. Environmental Protection Agency, Research Triangle Park, NC, November, 1985.
- Arand, J. K., Muzio, L. J., and Teixeria, D. P., "Urea Reduction of NO_x in Fuel Rich Combustion Effluents," US Patent No. 4,325,924, 1982.
- Atal, A., Steciak, J., and Levendis, Y. A., "Combustion and $\text{SO}_2\text{-NO}_x$ Emissions of Bituminous Coal Particles Treated with CMA," *accepted for publication in Fuel*, 1994.

- Beér, J., "Stationary Combustion: The Environmental Leitmotif," *Twenty-Second Symposium (International) on Combustion*, The Combustion Institute, Pittsburgh, PA, pp. 1-16, 1988.
- Bowman, C. T., "Kinetics of Pollutant Formation and Destruction in Combustion," *Progress in Energy and Combustion Science*, 1, pp. 33-34, 1975.
- Bowman, C. T., "Control of Combustion-Generated Nitrogen Oxide Emissions: Technology Driven by Regulation," *Twenty-Fourth Symposium (International) on Combustion*, The Combustion Institute, Pittsburgh, PA, pp. 859-878, 1992.
- Bruce, K. R., Gullet, B. K., and Beach, L. O., "Comparative SO₂ Reactivity of CaO Derived from CaCO₃ and Ca(OH)₂," *AIChE Journal*, 35(1), 37 (1989).
- Cole, J. A., Kramlich, J. C., Seeker, W. R., Silcox, G. D., Newton, G. H., Harrison, D. J., and Pershing, D. W., "Fundamental Studies of Sorbent Reactivity in Isothermal Reactors," Proceedings: 1986 Joint Symposium on Dry SO₂ and Simultaneous SO₂/NO_x Control Technologies, " EPRI CS-4966, December, 1986.
- Flagan, R. C., and Seinfeld, J. H., *Fundamentals of Air Pollution Engineering*, Prentice Hall, NJ, 1988.
- Freund, H., and Lyon, R. K., "The Sulfur Retention of Calcium-Containing Coal During Fuel-Rich Combustion," *Combustion and Flame*, 45, pp. 191-203, 1982.
- Greene, S. B., Chen, S. L., Clark, W. D., Heap, M. P., Pershing, D. W., and Seeker, W. R., "Bench-Scale Process Evaluation of Reburning

and Sorbent Injection for Infurnace NO_x/SO_x Reduction," Environmental Protection Agency, Research Triangle Park, NC, EPA/600/7-85/012, 1985.

- Hansen, R. K., and Saliman, S., "Survey of Rate Constants in the N-H-O System," in *Combustion Chemistry*, W. C. Gardiner, Ed., Springer-Verlag, New York, pp. 361-421, 1984.
- Levendis, Y. A., Zhu, W., Wise, D. L., and Simons, G. A., "The Effectiveness of Calcium Magnesium Acetate (CMA) as an SO_x Sorbent in Coal Combustion," *AICHE J.*, Vol. 39, No. 5, p. 761, 1993.
- Lyon, R. K., "Method for the Reduction of the Concentration of NO in Combustion Effluents Using Ammonia," US Patent No. 3,900,554, 1975.
- Myerson, A. L., "Method for Removing the Oxides of Nitrogen as Air Contaminants," US Patent No. 3,867,507, 1975.
- Miller, J. A., and Bowman, C. T., "Mechanism and Modeling of Nitrogen Chemistry in Combustion," *Progress in Energy and Combustion Science*, 15, 187, 1989.
- Sarofim, A. F., and Flagan, R. C., "NO_x Control for Stationary Combustion Sources," *Progress in Energy and Combustion Science*, 2, pp. 1-25, 1976.
- Yagiela, A. S., Maringo, G. J., Newell, R. J., and Farzan, H., "Update on Coal Reburning Technology for Reducing NO_x in Cyclone Boilers," American Power Conference, Chicago, 1991.

CHAPTER 6.

Custom-Blended Secondary Fuel and Sorbent Injection for Dual SO₂-NO_x Emission Control

Abstract

Estimations of operating costs suggested that the application of calcium and magnesium carboxylic acid salts for dual SO₂-NO_x reduction is practical only if a) the cost of the carboxylic acid salts can be significantly reduced; b) the utilization of the alkali earth metals by SO₂ is improved; and 3) part of the organic acid can be replaced by less expensive hydrocarbons for NO_x reduction. This study explored the latter requirement by investigating the dual reduction of SO₂-NO_x by combinations of calcium carboxylic acid salts and auxiliary hydrocarbons. The addition of lignite to achieve fuel-rich conditions with calcium propionate injected at a Ca/S molar ratio of ≈ 2 improved NO_x reduction from 35% to 80%. Including MgO in the above blend so that (Ca+Mg)/S=2 improved SO₂ capture from 15% to 30%. Blends of calcium formate and sucrose, injected at Ca/S=1 or 2 with varying amounts of sucrose to vary ϕ , showed increases in both NO_x and SO₂ reduction as ϕ increased. Excellent SO₂-NO_x reductions exceeding 90% were obtained by dry-injection of a blend consisting of calcium formate and poly(ethylene), warranting a more thorough investigation of replacing part of the expensive carboxylic acid by wastes that would otherwise be landfilled.

1 Introduction and Literature Review

Aliphatic carboxylic acid salts of Ca and Mg, e.g., calcium magnesium acetate (CMA), calcium formate (CF) and calcium propionate (CP), are effective agents for the simultaneous removal of SO_2 and NO_x emitted from the combustion of coal. Over 90% removal of these pollutants has been obtained by dry-injecting CMA in laboratory-scale experiments at temperatures near 1000°C in oxygen-lean atmospheres (3% O_2 , 12% CO_2 , 2000 ppm SO_2 and 1000 ppm NO in N_2) at a molar Ca/S ratio of 2 for a nominal 1 second residence time. Common thermodynamic and chemical kinetics windows wherein the dual reaction mechanisms are effective are defined by temperature (950 - 1150°C), residence time (1 - 4 s), and bulk equivalence ratio (ϕ between 1.1 and 1.3). The fuel-rich reaction zone is followed by a fuel-lean after-fire air zone, wherein occurs the oxidation of a) CO to CO_2 ; b) unburned HCs to CO_2 and water; and c) NH_3 to NO_x ; and the continued sulfation of Ca to CaSO_4 . Previous work exploring dual SO_2 - NO_x reduction quantified the contribution of Mg to SO_2 reduction by CMA (Steciak, et al., 1994d), showed that substantial amounts of CaCO_3 remain in the residues due to the incomplete decomposition of CaCO_3 to CaO – leading to the direct sulfation of CaCO_3 , and that the sulfation kinetics of the residues were bounded between those of pure CaO and pure CaCO_3 (Steciak, et al., 1994b, Steciak, et al., 1994d).

Commercially available carboxylic acid salts are expensive due to the cost of manufacturing the organic acid from natural gas. Research is underway at Northeastern University to develop manufacturing processes for extracting carboxylic acids from organic sources such as municipal waste, sewage sludge, and woody biomass. The simple calculations of operating costs that follow illustrate the economic challenge to improve the utilization of the alkali earth metals in the salts and reduce the cost of the organic components.

Consider a 1,000 MW plant burning coal with a thermal efficiency η_{th}

of 0.45. The thermal work input is thus $W_{th} = \frac{1000}{0.45} = 2,222$ MW. For a bituminous coal with a heating value of approximately $\Delta H_c = 30,000$ kJ/kg, the amount of coal that must be burned every day is

$$\dot{m}_c = W_{th}(\text{MW}) \frac{1}{\Delta H_c} \left(\frac{\text{kg}}{\text{kJ}} \right) \cdot 3600 \left(\frac{\text{sec}}{\text{hr}} \right) \cdot 24 \left(\frac{\text{hr}}{\text{day}} \right) = 6,400 \text{ metric tons of coal per day.}$$

If we assume that the coal contains 1.5% sulfur, then the mass of sulfur generated each day is $\dot{m}_s = 0.015 \cdot \dot{m}_c = 96$ metric tons; further assume that all of this sulfur is oxidized to SO_2 , i.e. 192 metric tons of SO_2 are emitted daily. For the control of SO_2 emissions (with a Ca utilization of 15% (Greene, et al, 1985)), an SO_2 sorbent must be injected at a Ca/S molar ratio of 2 to achieve 30% reduction. Assume that limestone (CaCO_3) is used. Hence, the mass of CaCO_3 that must be injected is $\dot{m}_{\text{CaCO}_3} = \dot{m}_s \cdot \frac{\text{Ca}}{\text{S}} \cdot \frac{MW_{\text{CaCO}_3}}{MW_S} = 600$ metric tons or $\approx 9\%$ of the mass of coal burned and, at \$ 20 per metric ton for limestone, \$ 12,000 per day is spent for SO_2 removal. Assuming that 20% of the coal is actually natural gas (methane) or lignite used as reburning fuel to remove NO_x , the daily cost of removing NO_x by reburning with natural gas is

$$0.20 \cdot \dot{m}_c \left(\frac{\text{m.ton}}{\text{day}} \right) \cdot \frac{1000\text{kg}}{\text{m.ton}} \cdot \frac{1 \text{ mol}}{16 \text{ g}} \cdot \frac{1000\text{g}}{\text{kg}} \cdot 75,000 \frac{\text{J}}{\text{mol}} \cdot \frac{\$2.5}{\text{GJ}} \cdot \frac{\text{GJ}}{10^9 \text{J}} = \$ 15,000 \text{ per day.}$$

The daily cost of reburning with lignite to remove NO_x is

$$0.20 \cdot \dot{m}_c \left(\frac{\text{m.ton}}{\text{day}} \right) \cdot \frac{1000\text{kg}}{\text{m.ton}} \cdot 17,200 \frac{\text{kJ}}{\text{kg}} \cdot \frac{\$1.5}{\text{GJ}} \cdot \frac{\text{GJ}}{10^6 \text{kJ}} = \$ 33,000 \text{ per day.}$$

Hence, the total daily cost of SO_2 and NO_x removal is \$ 27,000 to \$ 45,000, depending on the type of fuel used for reburning (natural gas and lignite, respectively), requires $\approx 30\%$ of the mass of fuel input to be injected, and only a third of the generated SO_2 is removed. NO_x removal of 70% has been reported by Greene, et al. (1985) for reburning with propane and as high as 70% in cyclone- fired boilers using natural gas as the reburning fuel (Yagiela, et al., 1991).

Now consider the application of CMA for the simultaneous removal of SO_2 and NO_x in the same power plant. At a Ca/S molar ratio of 2, the mass of CMA that must be injected is $\dot{m}_{\text{CMA}} = \dot{m}_s \cdot \frac{\text{Ca}}{\text{S}} \cdot \frac{MW_{\text{CMA}}}{MW_s} = 2,650$ metric tons per day, or $\approx 40\%$ of the mass of coal burned (the MW of CMA is 442 g/mol; note that this quantity of CMA corresponds to 33% of the mass of input fuel being used for NO_x and 8% for SO_2 removal). At a price of \$600/ton, this corresponds to \$ 1.6 million per day, or about 35 to 60 times more expensive than limestone and lignite or natural gas, respectively. A lighter carboxylic acid salt such as CP (186 g/mol) would still cost \$ 1.3 million per day, or 28 to 60 times more expensive than limestone and lignite or natural gas, respectively. Clearly, even though nearly all the SO_2 can be removed, the daily operational costs of using carboxylic acid salts must be reduced for practical application.

Boosting the utilization of the alkali earth metals in the carboxylic acid salts and reducing the cost of their organic component, either by manufacturing inexpensive carboxylic acids or by partial substitution of the organic by other traditional fuels such as natural gas or lignite, will reduce their cost. Assume a) a Ca/S molar ratio of 0.667 (or 50% utilization per alkali earth element in the CMA molecule); b) an order-of-magnitude reduction in the cost due to advanced techniques for generation of carboxylic acids from organic wastes; and c) substitution of natural gas or lignite for the additional hydrocarbons needed to achieve fuel-rich conditions for reburning. Under this scheme, the daily cost of CMA and lignite or natural gas is about twice the cost of limestone and natural gas, and about 30% more expensive than limestone and lignite; about 22% of the mass of input fuel would be injected for SO_2 and NO_x reduction.

Another interesting scheme would combine wet injection of a low molecular weight carboxylic acid (e.g., CF) with alternative fuels such as plastics in the municipal waste stream. The power plant would team 65% calcium utilization

obtained with wet injection (Steciak, et al., 1994c) with hydrocarbons that the plant might be *payed* to dispose of. The economics of this approach still require a drastic reduction in the price of carboxylic acids. Assuming that the price of CF can be lowered to one-tenth of the current price of \$ 600 per ton for CMA, the combination of CF and "free" hydrocarbons would be a third more expensive than limestone and natural gas, but 20% less expensive than limestone and lignite.

Other factors need to be considered. For example, deriving carboxylic acids from organic wastes diverts mass from landfills and captures "greenhouse" gases from natural decomposition that would otherwise be released into the atmosphere. The direct use of plastics and cellulosic materials – which would need to be finely shredded or ground – would divert considerable material from landfills. The inadvertent presence of chlorinated hydrocarbons, e.g., poly(vinyl chloride), might be tolerable because of the affinity of Ca for Cl to form CaCl_2 ¹ in the fuel-lean after-fire air zone (Dougherty, et al., 1993).

For the above reasons, we were interested in combining carboxylic acid salts with different amounts and types of hydrocarbons (e.g., an oxygen-containing hydrocarbon (sucrose) and a traditional fuel (lignite)). In addition, a few experiments were performed with poly(ethylene), a polymer found in quantity in the municipal waste stream ². The advantage of the custom-blended sorbents is the ability to deliver to a particular exhaust system, with its characteristic SO_2 and NO_x concentrations, a single injection of materials that have been optimized for the most efficient simultaneous removal of SO_2 - NO_x .

Previous work by Greene, et al. (1985) combined the injection of secondary fuels (various pulverized coals and propane) for NO_x reduction with the injection of calcium-based sorbents for SO_2 control. They concluded that the

¹ $\text{CaO} + 2 \text{H-C} + \text{C-Cl} + 4 \text{O}_2 \longrightarrow \text{CaCl}_2 + 4 \text{CO}_2 + \text{H}_2\text{O}$

²8 million tons of poly(ethylene) were discarded in 1990 (Wheatly and Levendis, 1993)

optimum location for sorbent injection was with the after-fire air because of increased reactivity of the calcined stone at 1000 - 1100°C (gas temperature at the location of after-fire air injection) compared to stone reactivity at 1400°C (gas temperature at the secondary fuel injection location). In our approach, the dual SO_2 - NO_x reduction can occur at the same temperature which is several hundred degrees Centigrade lower than the usual in-boiler secondary-fuel injection temperature for NO_x reduction in a “reburning” scheme (Wendt, et al., (1973)). Hence, loss of stone reactivity due to sintering is avoided and the simplicity of a single injection point is maintained – provided that one uses a secondary fuel that decomposes easily at the lower injection temperature. Incomplete sorbent calcination at injection temperatures below 1100°C and the lower rate of CaO sulfation at these temperatures are not detrimental because of the direct sulfation of CaCO_3 (Steciak, et al., 1994b, d; Tullin, et al., 1989; Snow, et al., 1988) and the sulfation of Mg if it is present in the stone.

2 Experimental Apparatus

The apparatus used was the same as that described in detail previously (Steciak, et al., 1994a-d, etc). Basically, the high-temperature bench-scale furnace consisted of an isothermal high temperature zone followed by a quenching zone wherein the temperature dropped at a rate of at least -350°C/sec (Figure 1). A capped stainless steel tube with end perforations facilitated the introduction of after-fire air at the end of the isothermal zone. All of the experiments described herein were conducted with dry-injected sorbents and solid hydrocarbons with a nominal residence time of 1 s (at 950°C, bulk $\text{Re} = 3000$ and $50\mu\text{m}$ particle $\text{Re} = 2.1$) in the isothermal zone. Sorbent was conducted pneumatically through a water-cooled injector to the beginning of the isothermal zone. For all experiments, the background gas partial pressures were 12% CO_2 ,

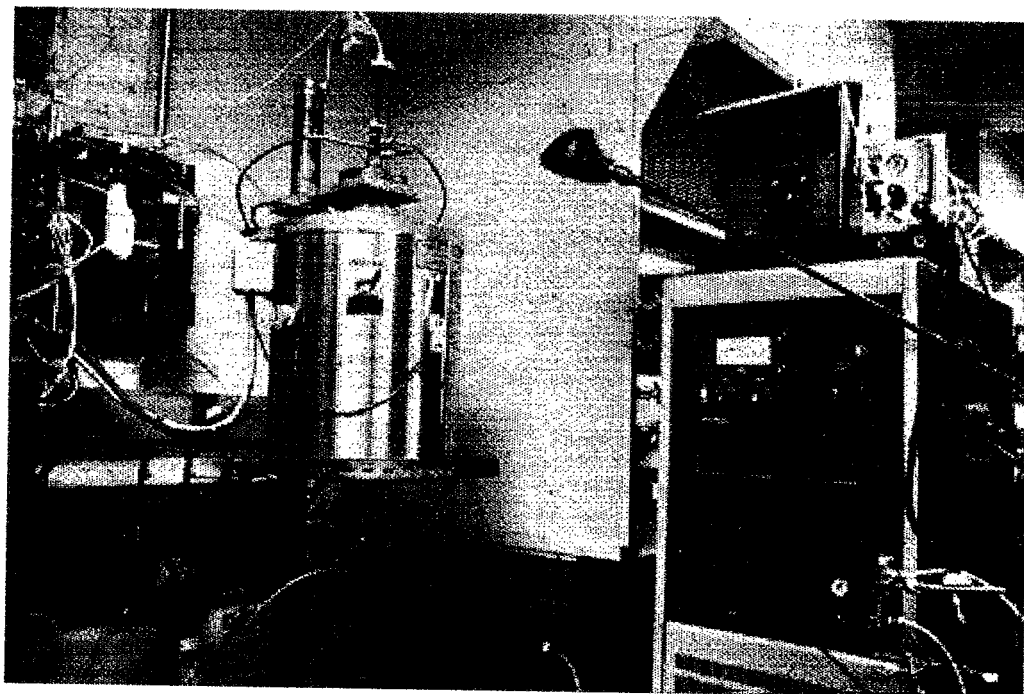


Figure 1: Experimental Apparatus

3% O₂, 2000 ppm SO₂ and 1000 ppm NO, balanced in N₂. Although NO alone was introduced to the furnace, the total NO_x (NO + NO₂) was monitored at the furnace exhaust. Other species monitored at the furnace exhaust were SO₂, CO, and CO₂.

3 Experimental Results and Discussion

Our goal was to determine the most efficient dual SO₂-NO_x reduction 'blend' of carboxylic acid salts and auxiliary hydrocarbons. The hydrocarbons we considered were lignite, sucrose and poly(ethylene). Lignite was chosen because it is a practical fuel, it has a relatively high volatility and thus had a greater likelihood of complete burnout at the gas temperatures and residence time used, and it had been shown to produce NH₃ under fuel-rich conditions (Chen, et al., 1982), thus the possibility of selective reactions between ammonia and NO_x near the 930°C temperature window of thermal de-NO_x (Lyon, 1975). Sucrose was chosen because it is an oxygen containing hydrocarbon and it was easy to work with experimentally; we used it to explore the effect of ϕ on SO₂-NO_x reduction under conditions where most of the hydrocarbons were outside – not a chemical part of – the carboxylic acid salts. Poly(ethylene) was chosen because it is found in abundance in the municipal waste stream.

3.1 SO₂-NO_x Reduction by CP and Lignite

a. SO₂ Reduction

The reductions of SO₂ and NO_x by CP, CP plus lignite and CP plus MgO and lignite are presented in Table I. When CP was injected at a Ca/S molar ratio ≤ 2.0 , the isothermal zone was fuel lean and the SO₂ reduction was low. This may have been due to poor dispersion of a small amount of sorbent. When lignite was added to create fuel-rich conditions, SO₂ capture changed

Table I. SO_2 - NO_x Reduction by CP and Lignite at 1050°C

Sorbent	$(\text{Ca} + \text{Mg})/\text{S}$	ϕ	SO_2 Red. (%)	Util. (%)	NO_x Red. (%)
CP	1.5	0.76	15	10	35
CP + lignite	1.8	2.3	15	8	80
CP + MgO + lignite	2	2.4	30	15	70

little. The addition of MgO doubled the SO_2 reduction, although the total alkali earth to sulfur molar ratio was kept ≤ 2 .

Results obtained by Greene, et al., in experiments using combinations of different sorbents and secondary fuels showed sulfur captures of 15% or 22% using calcitic limestone at a Ca/S molar ratio of 2 and propane as the secondary fuel. The difference in SO_2 capture was due to the location of the sorbent injection. A 15% SO_2 capture was obtained when the sorbent was injected with the secondary fuel at a location in their furnace where the gas temperature was $\approx 1400^\circ\text{C}$, whereas the 22% SO_2 capture occurred when the sorbent was injected with the after-fire air where the gas temperature was $\approx 1170^\circ\text{C}$. The difference in SO_2 capture was attributed to loss of stone reactivity at the higher injection temperature caused by sintering. The ϕ of the secondary fuel injection zone in that study was 1.1 and the residence times in the fuel-rich and after-fire zones were 0.4 sec. and ≈ 1 sec., respectively. The fuel-rich zone was not isothermal, but had a cooling rate of -575°C (the cooling rate of the after-fire zone was less than -200°C).

Greene, et al. (1985) concluded that SO_2 reduction was relatively insensitive to a variation in ϕ between 0.9 and 1.4. However, their data showing SO_2 and H_2S capture by calcitic limestone injected with the after-fire air at $\text{Ca}/\text{S}=2$ showed a clear, albeit slow, *decrease* in sulfur removal from 35%

to 25% as ϕ of the fuel-rich zone increased from 0.9 to 1.4. This trend is the same observed previously (Steciak, et al., 1994d) wherein, at an isothermal zone temperature of 950°C, the reduction of SO₂ measured downstream of the after-fire zone by carboxylic acid salts injected at Ca/S≈2.8 decreased from 75% at $\phi = 0.5$ to 50% at $\phi = 1.3$.

Another trend observed by Greene, et al. (1985) was the slow but measurable *improvement* of H₂S capture from 12% to 18% by calcitic limestone when both the sorbent and H₂S were **injected with the secondary fuel** at Ca/S=1 as ϕ increased from 0.9 to 1.4. This will be mentioned again below with the change in SO₂ capture by CF and sucrose as ϕ was varied.

Propane was the secondary fuel used by Greene, et al. (1985) to explore the dependence of sulfur capture on ϕ .

b. NO_x Reduction

When CP was injected at a Ca/S molar ratio ≤ 2.0 , the isothermal zone was fuel lean and the resulting NO_x reduction was low (Table I). This may have been due to poor dispersion of a small amount of sorbent. When lignite was added to create fuel-rich conditions, the NO_x reduction improved.

The NO_x reduction obtained by Greene, et al. (1985) using lignite injected at 1400°C was 50% at $\phi = 1.1$ and a NO_x background of ≈ 600 ppm. When the partial pressure of NO_x was reduced to ≈ 200 ppm, **no** NO_x reduction was obtained by secondary fuel injection. In both cases, the NO_x reduction *decreased* with increasing ϕ ; for the experiments with 190 ppm NO_x, NO_x production *increased* as ϕ decreased. The increase in NO_x production was attributed to the 1.11% nitrogen content of the lignite used in the experiments and the net production of NO_x above the background 190 ppm occurred for all of the nitrogen-containing coals used as secondary fuels. The reduction of NO_x by lignite improved when the after-fire zone temperature was cooled from $\approx 1100^\circ\text{C}$ to $\approx 900^\circ\text{C}$; the improvement was attributed to selective reduction

of NO by the amine radicals produced by lignite in the fuel-rich zone. When propane was injected as a secondary fuel, no net gain of NO_x was produced by this nitrogen-free fuel. At $\phi = 1.1$ with a NO_x partial pressure of ≈ 600 ppm, a maximum NO_x reduction of 55% occurred at an injection temperature of 1400°C and 70% at an injection temperature of 1560°C . The NO_x reduction tended to decrease, albeit slowly, as ϕ increased. This trend is the opposite of that observed previously (Steciak, et al., 1994d) wherein, at an isothermal zone temperature of 950°C , the reduction of NO_x measured downstream of the after-fire zone by carboxylic acid salts increased from 8% at $\phi = 0.5$ to 90% at ϕ between 1.1 and 1.3.

3.2 SO_2 - NO_x Reduction by CF and Sucrose

a. SO_2 Reduction

The reductions of SO_2 and NO_x by CF and sucrose are presented in Table II. When CF was injected at a Ca/S molar ratio ≈ 1.0 or ≈ 2.0 , the SO_2 capture and calcium utilization (Figure 2) *increased* as ϕ of the isothermal zone increased.

This trend is the opposite of that obtained by calcium carboxylic acid salts wherein ϕ was increased by using salts with increasing amounts of hydrocarbons bonded to Ca (Steciak. et al., 1994d), i.e., CF, CA and CP. A physical explanation of why these opposite trends occur may rest on the ease of decomposition of the hydrocarbon.

When most of the organic was imbedded within and bonded with the salt, local fuel-rich clouds enveloped the particles as the organic components gasified. As the fraction of organic within the salt increased, longer times were needed for gasification and subsequent diffusion of SO_2 to the calcined residues for heterogeneous sulfation.

When most of the organic was available outside the salt and decomposed

Table II. SO_2 - NO_x Reduction by CF and Sucrose at 1000°C

<u>Sucrose</u> Ca	Ca/S	ϕ	SO_2 Red. (%)	Util. (%)	NO_x Red. (%)
1.25	1.25	0.81	8	6	15
	2.5	0.87	10	11	35
	3.0	1.09	28	26	70
1.25	1.75	0.97	20	11	-
	1.6	2.16	68	31	65
	2.5	1.75	70	40	70

separately, as for the experiments listed in Table II and plotted in Figure 2, diffusion of SO_2 to the calcined residue was not hindered by an envelope cloud of gasifying hydrocarbons. Ca sulfation under fuel-rich conditions and fairly low temperatures may explain the role of the organic in SO_2 removal observed by Steciak, et al. (1994b). Precalcined CMA was injected at $(\text{Ca}+\text{Mg})/\text{S}=6$ and 750°C and failed to remove more than 10% of SO_2 . Injection of the precalcined CMA in combination with sucrose to achieve $\phi=1.3$ caused the same amount of SO_2 reduction as that obtained by raw CMA injected at the same $(\text{Ca}+\text{Mg})/\text{S}$ and ϕ .

It is not clear why Greene, et al. (1985) observed improvement of H_2S capture by calcitic limestone when both the sorbent and H_2S were injected with the secondary fuel.

b. NO_x Reduction

When CF was injected at a Ca/S molar ratio ≈ 1.0 or ≈ 2.0 , the NO_x reduction (Figure 3) *increased* as ϕ of the isothermal zone increased. This was consistent with the trend obtained by calcium carboxylic acid salts wherein ϕ was increased by using salts with increasing amounts of hydrocarbons bonded

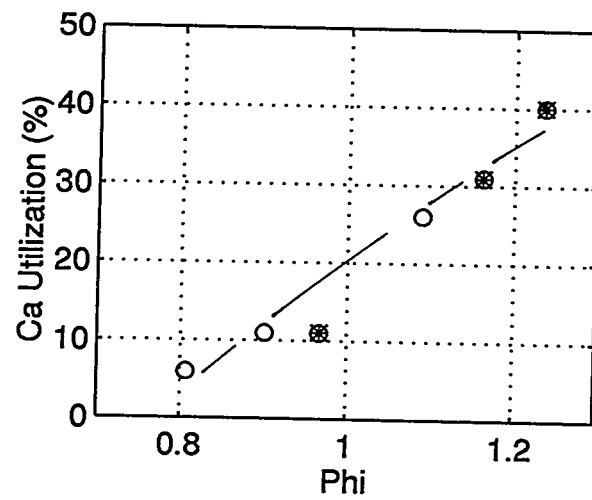


Figure 2: Ca utilization by CF and sucrose as a function of ϕ at 1000°C

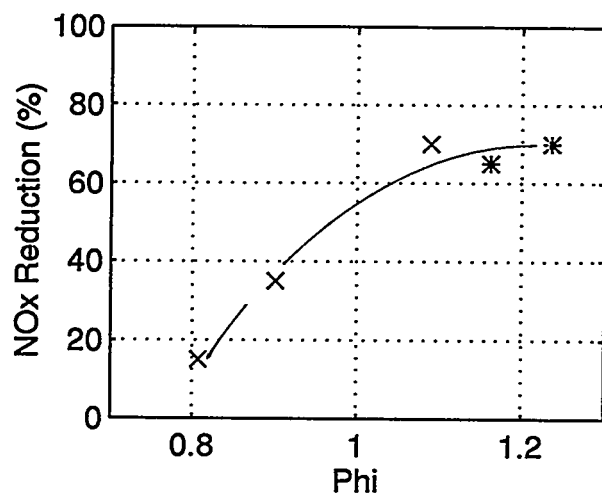


Figure 3: NO_x reduction by CF and sucrose as a function of ϕ at 1000°C

Table III. SO_2 - NO_x Reduction by CF and Poly(ethylene) at 1000°C

Zone	C/Ca	Ca/S	Iso. Zone ϕ	SO_2 Red. (%)	Util. (%)	NO_x Red. (%)
Isotherm.	12	2.2	2.0	98	45+	97
After-fire	12	2.2	2.0	98	45+	89

to Ca (Steciak, et al., 1994d), i.e., CF, CA and CP. While some NO_x reduction reactions are catalyzed by CaO (Steciak, et al. (1994a), most selective and non-selective reactions occur in the gas phase and would not be affected by diffusion through local fuel-rich clouds. The trend of improving NO_x reduction with increasing ϕ in Figure 3 was the opposite of that observed by Greene, et al. (1985). The explanation for the difference may lie in the significant difference in gas temperature between the experiments of Greene, et al. (1985) and Figure 3 (1400 vs. 1000 °C, respectively). The lower temperature reactions may allow for the selective reduction of NO by NH_3 formed during the fuel-rich decomposition of the organics. Some NH_3 was measured in the isothermal reaction zone during NO_x reduction by CP (Steciak, et al. (1994)) and nearly all of it oxidized to NO_x in the after-fire air zone.

3.3 SO_2 - NO_x Reduction by CF and Poly(ethylene)

a. SO_2 Reduction

Nearly 100% reduction of SO_2 was obtained by a blend of CF and poly(ethylene) at 1000°C at a $\text{Ca/S}=2.2$, $\phi=2.0$ and $\text{C/Ca}=12$ (or one mole of $[-\text{CH}_2-]_{10}$ per mole of Ca), as listed in Table III. The addition of after-fire air had no effect on SO_2 reduction.

b. NO_x Reduction

Nearly 100% reduction of NO_x was obtained by the same blend of CF and poly(ethylene), as listed in Table III. The addition of after-fire air lowered NO_2 reduction to 89%, suggesting that NH_3 or HCN products from the fuel-rich reaction zone were oxidized back to NO_x .

The excellent SO_2 - NO_x reduction demonstrated by this blend of carboxylic acid salt and plastic is intriguing and warrants the full investigation of blends of different carboxylic acid salts and other plastics.

4 Conclusions and Recommendations

1. Simple calculations of operating costs suggest that application of the carboxylic acid salts for dual SO_2 - NO_x reduction could become competitive if their price is lowered significantly, if the utilization of the alkali earth metals is optimized, and if part of the expensive carboxylic acids could be replaced with less expensive hydrocarbons such as lignite or even waste plastics.
2. The reduction of SO_2 by combinations of calcium carboxylic acid salts and hydrocarbons injected into the reaction zone increased as ϕ increased. This trend opposed that found previously by Steciak, et al. (1994d) wherein the reduction of SO_2 by carbon carboxylic acid salts decreased as ϕ increased. The physical explanation may rest on the ease of decomposition of the hydrocarbon.

When most of the organic was bonded within the salt, local fuel-rich clouds that could be extremely fuel-rich enveloped the particles as the organic components gasified and opposed the diffusion of SO_2 to the particle. When most of the organic was available outside the salt and decomposed separately, diffusion of SO_2 to the calcined residue was not hindered by an envelope cloud of gasifying hydrocarbons.

3. The reduction of NO_x by calcium carboxylic acid salts increased as ϕ increased regardless of whether the increase in ϕ was due to an increase in hydrocarbons bonded to the Ca or injected into the reaction zone. This trend suggests that selective reduction of NO could occur in the by amine radicals that were produced in the fuel-rich zone as the hydrocarbons decomposed. This selective reduction would be in addition to the non-selective reduction of NO_x by HC radicals.
4. Excellent $\text{SO}_2\text{-NO}_x$ reduction was obtained by a dry-injected blend of CF and poly(ethylene). Further investigation of carboxylic acid salt-plastic blends are warranted.
5. Dual $\text{SO}_2\text{-NO}_x$ reduction by combinations of wet-sprayed carboxylic acid salts and different plastics should be investigated. Wet-spraying achieves high Ca utilization for efficient SO_2 removal. The use of waste plastics as sacrificial hydrocarbons for the reduction of NO_x diverts significant amounts of material from landfills. The presence of Ca in the reaction zone may also remove Cl, a decomposition product of chlorinated hydrocarbons, in the form of CaCl_2 . The combination of wet-sprayed carboxylic acid salts and waste plastics may be the most economical and advantageous scheme for $\text{SO}_2\text{-NO}_x$ reduction, providing that the cost of the carboxylic acid salts can be significantly reduced and the plastics can be shredded or ground to facilitate quick decomposition in the reaction zone.

5 Acknowledgments

This work was supported by U.S. Dept. of Energy University Grant DE-FG22-92PC92535.

6 References

- Chen, S. L., Clark, W. D., Heap, M. P., Pershing, D. W., and Seeker, W. D. (1982) NO_x Reduction by Reburning With Gas and Coal - Bench Scale Studies. *Proceedings of the Joint Symposium on Stationary Combustion NO_x Control.*
- Doughty, R. C., and Collazo-Lopez, H. (1987). Reduction of Organochlorine Emissions from Municipal and Hazardous Waste Incinerators. *Environmental Science and Technology*, **21**, 602 - 604.
- Greene, S. B., Chen, S. L., Clark, W. D., Heap, M. P., Pershing, D. W., and Seeker, W. R. (1985) Bench-Scale Process Evaluation of Reburning and Sorbent Injection for In-furnace NO_x/SO_x Reduction. Environmental Protection Agency, Research Triangle Park, NC, EPA/600/7-85/012.
- Lyon, R. P. (1975) Method for the Reduction of the Concentration of NO in Combustion Effluents Using Ammonia. *U.S. Patent No. 3,900,554.*
- Snow, M. J. H., Longwell, J. P., and Sarofim, A. F. (1988) Direct Sulfation of Calcium Carbonate. *Ind. Eng. Chem. Res.* **27**, 268-273.
- Steciak, J., Zhu, W., Levendis, Y. A., and Wise, D. L. (1994a) The Effectiveness of Calcium (Magnesium) Acetate and Calcium Benzoate as NO_x Reduction Agents in Coal Combustion. *Accepted for publication in Combustion Science and Technology.*
- Steciak, J., Levendis, Y. A., and Wise, D. L. (1994b) The Effectiveness of Calcium Magnesium Acetate as a Dual SO₂-NO_x Emission Control Agent. *Submitted for publication.*
- Steciak, J., Levendis, Y. A., Wise, D. L., and Simons, G. A. (1994c) Reduction of Combustion-Generated SO₂-NO_x by Fine Mists of CMA. *19th*

International Conference on Coal Utilization and Fuel Systems, Clearwater, Florida.

- Steciak, J. Levendis, Y. A., Wise, D. L., and Simons, G. A. (1994d) Dual SO₂-NO_x Reduction by Calcium Salts of Carboxylic Acids. *Submitted for publication*.
- Tullin, C., and Ljungström, E. (1989) Reaction Between Calcium Carbonate and Sulfur Dioxide. *Energy and Fuels*. **3**, 284 - 287.
- Wendt, J. O. L, Sternling, C. V., and Matovich, M. A. (1973) Reduction of Sulfur Trioxide and Nitrogen Oxides by Secondary Fuel Injection. *Fourteenth Symposium (International) on Combustion*. pp. 897 - 904, The Combustion Institute, Pittsburgh.
- Wheatly, L., Levendis, Y. A., and Vouros, P. (1993) Exploratory Study on the Combustion and PAH Emissions of Selected Municipal Waste Plastics. *Environmental Science and Technology*. **27**, 2885 - 2895.
- Yagiela, A. S., Maringo, G. J., Newell, R. J., and Farzan, H. (1991) Update of Coal Reburning Technology for Reducing NO_x in Cyclone Boilers. *American Power Conference*.

CHAPTER 7.

Overall Summary

A study was conducted to determine the efficacy of carboxylic calcium and magnesium salts for the simultaneous removal of SO_2 and NO_x in oxygen-lean atmospheres. Experiments were performed in a high-temperature, laboratory-scale furnace which simulated the post-flame environment of a coal-fired boiler by providing similar temperatures and partial pressures of SO_2 , NO_x , CO_2 and O_2 . The salts tested included calcium magnesium acetate (CMA, $\text{CaMg}_2(\text{CH}_2\text{COOH})_6$), calcium acetate (CA, $\text{Ca}(\text{CH}_2\text{COOH})_2$), magnesium acetate (MA, $\text{Mg}(\text{CH}_2\text{COOH})_2$), calcium formate (CF, $\text{Ca}(\text{COOH})_2$), calcium propionate (CP, $\text{Ca}(\text{CH}_2\text{CH}_2\text{COOH})_2$), and calcium benzoate (CB, $\text{Ca}(\text{C}_7\text{H}_5\text{O}_2)_2$).

When injected into a hot environment, the salts calcined and formed highly porous cenospheres. Residual MgO and/or CaCO_3 and CaO reacted heterogeneously with SO_2 to form MgSO_4 and/or CaCO_4 . The organic components gasified and reduced NO_2 to N_2 effectively in moderately fuel-rich atmospheres.

On a Ca/S molar ratio basis, CMA was found to be the most effective dual SO_2 - NO_x reduction agent. Dry-injected CMA particles at a Ca/S ratio of 2 and bulk equivalence ratio ϕ of 1.3 removed 90% of SO_2 and NO_x at gas temperatures $\geq 950^\circ\text{C}$ in atmospheres containing 3% O_2 , 12% CO_2 , 2000 ppm SO_2 , and 1000 ppm NO_x during a ≈ 1 s residence time in the isothermal zone of the furnace.

The role of Mg during rapidly quenched experiments at gas temperatures $\leq 950^\circ\text{C}$ was quantified. In the isothermal zone, on a per-mole basis, Ca contributed between 20 and 30%, and Mg contributed between 10 and 15%, to SO_2 reduction during a 4 s residence time. Ca was essentially inert in the furnace quenching zone, while Mg continued to sorb SO_2 as the gas temperature cooled at a rate of -130°C/sec . Hence, the removal of SO_2 by CMA could continue for nearly the entire residence time of emissions in the exhaust stream

of a power plant.

It can be expected that isothermal zone temperatures 950°C – including temperatures above 1270°C, the stability limit for CaSO_4 – could lead to temperatures that are high enough to favor Ca sulfation kinetics in the region of the furnace where gas temperature cooled at a rate of -130°C/sec. Essentially no SO_2 was emitted during the combustion of CMA-treated pulverized coal in air at furnace gas temperatures of 1180°C. During these experiments, the temperature of the volatile and char phase of coal particles treated with CMA were 2130 and 1730°C, respectively (Appendix I).

At gas temperatures below 800°C, the organic components of the salts did not completely gasify during the residence time in the furnace. Ca was transformed to CaCO_3 and/or bound organically; the organically bound Ca would be unavailable for reaction with SO_2 . At temperatures between 900 to 1150°C, Ca was found in the forms of CaCO_3 and/or CaO . The composition of the calcined salts and the availability of Ca was used to interpret the results of a cenosphere sulfation model. The sulfation kinetics of Ca-containing residues were found to be bounded by those of pure CaO and pure CaCO_3 .

The high solubility of the salts, compared with slaked lime ($\text{Ca}(\text{OH})_2$) or limestone (CaCO_3) (e.g., 30 g/100 cc for CMA vs. 0.85 g/100cc for slaked lime and 0.0015 g/100cc for limestone) makes them excellent candidates for wet injection. Fine mists of CMA, produced with an aerosol generator and sprayed in the furnace at temperatures between 850 and 1050°C, removed 90% of SO_2 at a Ca/S molar ratio of 1, about half of the amount used in the dry injection experiments. About 15% of the SO_2 was scrubbed by water alone. When CMA was sprayed at a Ca/S ratio of 1, the NO_x reduction chemistry was not affected by the presence of water, i.e., the same reduction efficiency was achieved as with dry injection (25 - 30%).

Because the efficiency of NO_x removal by secondary fuel injection is a func-

tion of the initial partial pressure of NO, future experiments should determine the SO_2 - NO_x reduction efficacy of the carboxylic acid salts when the initial NO partial pressure is 300 ppm and below.

Additional research is needed to improve the efficiency and reduce the cost of the relatively expensive carboxylic acid salts as dual SO_2 - NO_x reduction agents. One suggestion is combining wet injection of the salts (with a Ca utilization of – or perhaps even higher than – 65%) with less expensive reburning fuels such as lignite or even polymers such as polyethylene which could be extracted from the municipal waste stream.

APPENDIX II.

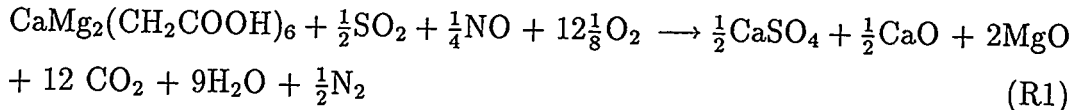
Determination of the Bulk Equivalence Ratio, ϕ

The bulk or average equivalence ratio, ϕ , is defined as the ratio of the actual fuel-to-oxidant ratio to the stoichiometric fuel-to-oxidant ratio. If ϕ is less than one, more than enough oxidant is present to react with all the fuel and the reaction conditions are termed fuel-lean. If ϕ is equal to one, exactly enough fuel and oxidant are present for the reactions to go to completion. This condition is called stoichiometric. When ϕ is greater than one, more than enough fuel is present to react with all the oxidant, and this condition is called fuel-rich. It is important to note that the bulk ϕ is the same as the actual ϕ in a reactor only if the reactants are perfectly mixed. Usually this is not the case and pockets of fuel-rich and fuel-lean conditions can exist regardless of the bulk ϕ . Nonetheless, the calculation of ϕ is useful practically since it indicates trends and can guide burner design to control emissions.

In the furnace used for the experiments with dual SO_2 - NO_x reducing agents, the sorbents were either dry- or wet-injected. In both cases, the sorbents were injected directly into the hot isothermal reaction zone (via pneumatic transport through a water-cooled injector) which contained a mixture of SO_2 and NO . The sorbents mixed with the gases in the furnace. Each particle or droplet briefly sustained an envelope of gasifying hydrocarbons, creating fuel-rich conditions within the envelope. When gasification was complete, SO_2 had to diffuse into the interior pores of the resulting cenospheres. During the sulfation of cenospheres containing CaCO_3 , CO_2 was released as a product and had to diffuse out of the interior pores. Even when a blend of SO_2 and NO was used to transport the sorbents to the isothermal zone in order to pre-mix the sorbents and the gases, considerable local diffusion and mixing occurred because of gasification and sulfation. Hence, the value of calculating ϕ was

simply to observe trends and note changes in sulfation and NO_x reduction efficiency as overall conditions change from fuel-lean to fuel-rich.

Oxygen was present in most of the sorbents as well as in SO_2 , NO , and the background gas. For CMA injected at a molar Ca/S ratio of 2 in an atmosphere containing 2000 ppm SO_2 , 1000 ppm NO and unlimited O_2 , the overall stoichiometry to reduce NO to N_2 and form CaSO_4 from SO_2 and Ca was described by the following global reaction:



For each mole of fuel (CMA), the number of moles of oxygen in the reactants was $6 + \frac{1}{2} + \frac{1}{8} + 12\frac{1}{8} = 18\frac{3}{4}$. Hence, the stoichiometric fuel-to-air ratio was $f_s = \frac{\text{MW}_{\text{CMA}}}{18\frac{3}{4}\text{MW}_{\text{O}_2}} = 0.737$, i.e., one gram of O_2 was needed with each 0.737 g of CMA to completely convert SO_2 to CaSO_4 and NO to N_2 - with unreacted CaO and MgO left over.

The actual fuel-to-oxidant ratio in the isothermal reaction zone was quite different. The molar flow of O_2 in the sorbent, SO_2 , NO and the background gas were determined first. For each gas, its molar inflow was

$$p_{\text{gas}} \dot{V} \frac{1}{22.4 \text{lit/mol}} \frac{273}{295} \quad (1)$$

where p_{gas} was the partial pressure of the gas (in N_2) and \dot{V} its volumetric flow rate. Because SO_2 and NO were introduced into the furnace at a volumetric rate of 1 lpm at room temperature, and O_2 at a rate of 2 lpm, the partial pressure of all of the gases at the furnace inlet was higher than that in the furnace because of dilution to achieve the desired final concentration. For CMA injected at a Ca/S molar ratio of 2 in an atmosphere containing 2000 ppm SO_2 , 1000 ppm NO and 3% O_2 , the inlet partial pressures were 6000 ppm SO_2 , 3000 ppm NO , and 4.5% O_2 . Hence, the total mass inflow of O_2 was

$$\dot{m}_{\text{O}_2} = (\dot{n}_{\text{SO}_2} + \frac{1}{2}\dot{n}_{\text{NO}} + \dot{n}_{\text{O}_2} + \dot{n}_{\text{O}_2 \text{inCMA}}) \cdot \text{MW}_{\text{O}_2} \quad (2)$$

where \dot{n} is the molar flow rate and

$$\dot{n}_{O_2 \text{ in CMA}} = 6 \cdot Ca/S \cdot \dot{n}_{SO_2} \quad (3)$$

since there were 6 moles of O_2 for each mole of CMA. The mass inflow of CMA was

$$\dot{m}_{CMA} = MW_{CMA} \cdot Ca/S \cdot \dot{n}_{SO_2} \quad (4)$$

This resulted in an actual fuel-to-oxidant ratio of $f_a = 0.935$, i.e., 0.935 g of CMA was provided with each gram of O_2 in an attempt to convert SO_2 to $CaSO_4$ and NO to N_2 . Whether or not this amount of O_2 was sufficient was determined by the equivalence ratio:

$$\phi = \frac{f_a}{f_s} = \frac{0.935}{0.737} = 1.27$$

Here, $\phi > 1$; hence, the overall reaction conditions were fuel-rich and insufficient O_2 was provided for the complete conversion of the reactants to the products listed in R1. In the experiments, fuel-rich conditions resulted in copious formation of CO and trace concentrations of H_2S , HCN and NH_3 . The addition of afterfire air oxidized CO to CO_2 , H_2S to SO_2 , and HCN and NH_3 to NO and thus lowered the overall SO_2 - NO_x reduction efficiency. The loss of dual SO_2 - NO_x reduction efficiency was significant for $\phi > 1.3$ (Chapter 5).

The bulk equivalence ratios for the other sorbents and different Ca/S molar ratios were calculated in a similar manner.

Notation

SYMBOL	DESCRIPTION	UNITS
f_a	actual fuel-to-oxidant ratio	-
f_s	stoichiometric fuel-to-oxidant ratio	-
MW	molecular weight	$\frac{g}{mol}$
\dot{m}	mass flow rate	$\frac{g}{min}$
\dot{n}	molar flow rate	$\frac{mol}{min}$
p	partial pressure	atm

\dot{V}	volumetric flow rate	$\frac{\text{lit}}{\text{min}}$
ϕ	equivalence ratio	-

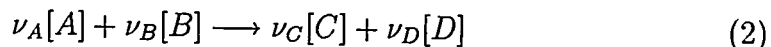
APPENDIX III.

Chemical Thermodynamics and Chemical Kinetics Calculations

Whether or not a chemical reaction was thermodynamically possible over a particular temperature range was determined by calculating the change in the Gibbs free energy per mole, ΔG (or the chemical potential), for that reaction. For an individual species,

$$\Delta G_f = h_o + \Delta h - T\Delta s \quad (1)$$

where h_o is the enthalpy of formation at 298 K, Δh is the enthalpy change between 298K and temperature T, and s is the absolute entropy. Occasionally, thermodynamic data sources - especially ones published in recent years - tabulated ΔG_f directly, but Eqn. 1 was used most frequently. The thermodynamic data sources used are listed below. For a particular chemical reaction



where ν_i are the stoichiometric coefficients and $[i]$ denotes concentration of species i , the change in Gibbs free energy is

$$\Delta G = \sum \nu_p \Delta G_{f,p} - \sum \nu_r \Delta G_{f,r} = \nu_C \Delta G_{f,C} + \nu_D \Delta G_{f,D} - (\nu_A \Delta G_{f,A} + \nu_B \Delta G_{f,B}) \quad (3)$$

If ΔG is negative, the reaction is spontaneous at all T. Also,

$$\Delta G = -RT \ln(K(T)) \quad (4)$$

where R is the ideal gas constant and $K(T)$ is the equilibrium constant defined by

$$K(T) = \frac{y_C^{\nu_C} y_D^{\nu_D}}{y_A^{\nu_A} y_B^{\nu_B}} \frac{p}{p_{ref}}^{\nu_C + \nu_D - \nu_A - \nu_B} \quad (5)$$

where y_i are the species mole fractions and p is pressure. Hence, the equilibrium constant can be calculated if ΔG is known. It also follows that, if

$\log_{10}(K(T))$ is positive, the reaction is spontaneous. The Gibbs free energy change was calculated using tabulated thermodynamic data from 700 to 1700K (427 - 1427°C) for a number of reactions in Chapters 2 and 5.

Knowledge of the rate of reaction was needed to determine how fast a reaction would occur, given that it was spontaneous over the temperature range of interest. Kinetics and thermodynamics are linked by the equilibrium constant and the rate constants for a reaction:

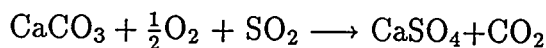
$$K(T) = \frac{k_f}{k_r} \quad (6)$$

where k is the rate constant, the subscripts f and r refer to the forward and reverse reactions, respectively, and k is assumed to follow the Arrhenius equation:

$$k = A \cdot \exp\left(-\frac{E_a}{RT}\right) \quad (7)$$

where A is the pre-exponential factor and E_a is the activation energy. Thus, if the forward rate constant is known, the reverse constant can be calculated, and vice versa.

For example, the reaction rate constant for the direct sulfation of CaCO_3 :



was provided by Snow, et al. (1988) as

$$k_f = 71.8 \cdot \exp\left(-\frac{15,300}{1.987T}\right) \frac{\text{cm}}{\text{sec}} \quad (8)$$

To convert this to the same scale used in the sulfation model (Simons, et al., 1987) used in Chapter 5, the pre-exponential factor 71.8 was modified by

$$A' = 71.8 \frac{MW_{\text{SO}_2}}{RTp_{\text{SO}_2}} \frac{g}{\text{cm}^2 \cdot \text{sec} \cdot \text{atm}} \quad (9)$$

so that

$$k' = 71.8 \frac{MW_{\text{SO}_2}}{RTp_{\text{SO}_2}} \cdot \exp\left(-\frac{15,300}{1.987T}\right) \quad (10)$$

A straight line fit to a plot of $\ln(k')$ vs. $1/T$ yielded a new effective pre-exponential factor ($A'' = 10.76$) and activation energy ($E_a' = -13,440$ cal/mol) that were used in the sulfation model. The reverse reaction rate constant was calculated using Eqn. 6.

REFERENCES

- Simons, G. A., Garman, A. R., and Boni, A. A., "The Kinetic Rate of SO_2 Sorption by CaO ," *AICHE Journal*, **33**, 211, 1987.
- Snow, M. J. H., Longwell, J. P., and Sarofim, A. F., "Direct Sulfation of Calcium Carbonate," *Industrial and Engineering Chemical Research*, **27**, 268, 1988.

THERMODYNAMIC DATA SOURCES

- Barin, I., "Thermochemical Data of Pure Substances," VCH Publishers, NY, NY, 1989.
- Chase, et al., "JANAF Thermochemical Tables," *J. Phys. Chem. Ref. Data*, **14**, Suppl. 1, 1985.
- Gurvich, L. V., Veyts, I. V., Alcock, C. B., and Iorish, V. S., Eds., *Thermodynamic Properties of Individual Substances*, Fourth Edition, Hemisphere, NY, NY, 1991.
- Kee, R. J., Rupley, F. M., and Miller, J. A., "The Chemkin Thermodynamic Data Base," SAND87-8215B, Sandia National Laboratories, Albuquerque, NM, 1990.
- Lide, D. R., Ed., *CRC Handbook of Chemistry and Physics*, 73rd Edition, CRC Press, Ann Arbor, MI, 1992-93.

- Yaws, C. L., *Thermodynamic and Physical Property Data*, Gulf Publishing Company, London, 1992.

Notation

SYMBOL	DESCRIPTION	UNITS
A	pre-exponential factor	varies
E_a	activation energy	$\frac{cal}{mol}$
ΔG	Gibbs free energy change	$\frac{kJ}{kmol}$
h_o	enthalpy of formation	$\frac{kJ}{kmol}$
Δh	enthalpy	$\frac{kJ}{kmol}$
k	reaction rate constant	varies
$K(T)$	equilibrium constant	-
p	pressure	atm
R	ideal gas constant	$0.080206 \frac{atm \cdot lit}{mol \cdot K}$ or $1.987 \frac{cal}{mol \cdot K}$
s	absolute entropy	$\frac{kJ}{kmol \cdot K}$
T	temperature	K
y	mole fraction	-
ν	stoichiometric coefficient	mol